Observation of the Expansion Behavior and Quantitative Evaluation of Elastic Recoil of a Balloon-Expandable Stent in Three Dimensions Using a Micro-CT system

Futoshi MORI [(1) (2)], Toshio NAKAYAMA [(3)], Teruo MATSUZAWA [(4)], Makoto OHTA [(5)*]

(1) Center for Integrated Disaster Information Research, Interfaculty Initiative in Information Studies, The University of Tokyo, 1-1-1 Yayoi Bunkyo-ku, Tokyo 113-0032, JAPAN: f-mori@eri.u-tokyo.ac.jp
(2) Earthquake Research Institute, The University of Tokyo, Tokyo, JAPAN
(3) Graduate School of Biomedical Engineering, Tohoku-University, Sendai, JAPAN
(4) Research Center for Simulation Science, Japan Advanced Institute of Science and Technology, Ishikawa, JAPAN
(5) Institute of Fluid Science, Tohoku-University, Sendai, JAPAN

Abstract. Percutaneous transluminal coronary angioplasty (PTCA) with stent implantation is widely used for the treatment of coronary stenosis. However, restenosis after stent implantation frequently reported by intravascular ultrasound evaluation. This may occur because of the reduced luminal area after implantation, insufficient stent expansion, or by the elastic recoil of the stent (ERS). Quantitative evaluation of stent expanding should provide further information on how to decrease the incidence of re-stenosis. Many previous studies have observed stent properties in 2D. However, the stent geometry is changed in 3D space, and 3D measurements will provide further information on factors such as the risk for asymmetric ERS. We performed 3D reconstruction using high spatial resolution images obtained with a Micro-CT system to observe the 3D expansion behavior of a test stent and quantitatively evaluate ERS. The

* Corresponding author: Makoto Ohta, Institute of Fluid Science, Tohoku-University, 2-1-1 Katahira, Aoba-ku, Sendai, 980-8577, JAPAN, Tel/Fax: +81 22 2175309, E-mail: ohta@biofluid.ifs.tohoku.ac.jp

expansion behavior of each structural component of the stent varied, as did the ERS and eccentricity. ERS ranged from 2.4% to 9.2% during observation form proximal and distal positions in each component. The greatest difference in ERS between 2D and 3D measurements was 5.2%. 3D measurements provide more information on ERS than 2D measurements. Our result shows the importance of the observation, and the evaluation by three dimensions.

Keywords: Three dimensional, Micro-CT, Expansion behavior, Elastic recoil of stent, Balloon-expandable stent

1. Introduction

Disorders associated with ischemic heart disease, such as angina and myocardial infarction, are well known, and the mortality rate from ischemic heart disease is high. The disease results from stenosis or blockage of the coronary artery that supplies oxygen and nourishment to the cardiac tissue [1].

Percutaneous transluminal coronary angioplasty (PTCA) is a minimally invasive procedure used to open up the blocked coronary artery and allow unobstructed circulation of blood to the heart muscle [2]. However, the dilated blood vessel is deflated immediately by approximately 50% following this procedure because of the elastic properties of the vessel [3]. This deflation can be prevented by stent implantation. A

stent is a therapeutic device that has a coil or cylindrical shape. PTCA with stent implantation can cause greater expansion of the lumen than PTCA alone. Moreover, PTCA with stent implantation can decrease the risk of acute coronary occlusion and restenosis as well as overcome the disadvantages associated with PTCA [4]. However, shrinkage of vascular has been observed by intravascular ultrasound (IVUS) [5] and is known as Elastic recoil (ER). And optical coherence tomography is also used for ER [6-8]. This ER cause may be shrinkage of the stent called as elastic recoil of the stent (ERS). And the ERS may lead to restenosis.

Drug-eluting stent (DES) is used to prevent the restenosis. DES suppresses the neointimal hyperplasia, however in-stent restenosis after DES implantation still occur [9]. Hwang et al. have shown that nonuniform circumferential stent strut distribution affects local drug concentration [10]. Therefore, it is important that the characteristics of stents be studied further.

Several parameters, such as the size or form of the mesh and metal used, characterize the mechanical behavior of the stent and may influence ERS. ERS will occur when the area of plasticity deformation is exceeded. Barragan et al. measured ERS of 23 coronary stents in two dimensions (2D) using an optical gauging system [11]. Many stents have various ERS behavior, and the extent of ERS may depend on the design of the stent.

Tanimoto et al. evaluated ERS between the bioabsorbable everolimus-eluting stent and the everolimus-eluting metallic stent [6]. In vivo acute ERS of the bioabsorbable everolimus-eluting stent is slightly larger but insignificantly different from that of the everolimus-eluting stent. Yamamoto et al. measured the cross-sectional area of stents by IVUS and confirmed the luminal area in 2D [5]. Moreover, the stent of geometrical parameters has been demonstrated for relation to adverse clinical outcomes. Otake H et al. observed the stent eccentricity index (SEI) [12] and was clarified that SEI is related as one of the factors for generation of thrombus. They also described that asymmetric stent expansion leads to thrombosis. However, stent expansion occurs in the three-dimensional (3D) space, and therefore, evaluation of ERS in 2D will not provide complete information on stent expansion behavior.

Sun Z et al. observed difference between 2D and 3D using multislice CT [13]. However, the normal tomography occur the artifact from stent. Therefore, the accurate information is still not satisfied. Recently, several researches observe using OCT [14][15]. An OCT image provides a detailed assessment of plaque characteristics and results of stenting, because of its high resolution. However, OCT is still low resolution for the stent strut. Gurmeric S et al. showed the reconstructed stent shape using OCT images [16]. This stent shape is not reproduced in detail. Therefore, we used Micro-CT

system. The micro focus X-ray computed tomography (Micro-CT) system is a potential tool for 3D reconstruction of small implants; it generates high spatial resolution images. Ohta et al. showed that a stent could be reconstructed in 3D [17], and Connolley et al. observed a stent in a simple mock artery with stenosis using the Micro-CT system [18]. These studies reproduced the stent shape in detail.

In this study, we performed 3D reconstruction using the Micro-CT system to observe stent expansion behavior and quantitatively evaluate ERS.

2. Materials and Methods

2.1 Materials

2.2.1 Micro-CT System

Figure 1 shows a schematic diagram of the experimental Micro-CT system (SMX-100CT- SV3; Shimadzu Co., Japan) that generates high spatial resolution images. Table.1 details the operating conditions of the Micro-CT system. The operating conditions were determined after several preliminary tests to decrease the effects of stent artifacts.

2.1.2 Balloon Expandable Stent

The coronary stent (Terumo Co., Japan) shown in Figure 2 was used for measuring ERS. This stent consists of stent, a balloon for expansion, and a rapid exchange type delivery catheter. Its unique 4-cell mono-link structure has been shown to provide greater track-ability, flexibility, and conformity to the vasculature. In addition, the diamond-spaced cellular design may provide exceptional radial strength. The stent comprises 6 structural components. The upper panel in Figure 2 shows the balloon-expandable stent at 0.0 atm, and the lower panel shows the stent at 8.0 atm. Each of the structural components is referred to by a number ranging from 1 to 6. Moreover, the proximal and distal points at each ends of each structural component were defined. d1 in the coronal plane and d2 in the sagittal plane were connected to the opposite point in the cross-section of the stent shown in Figure 3.

By inflating the balloon, the stent can be expanded to a specific diameter of 2.5×10^{-3} m, which is equal to the internal diameter at a specific pressure of 8.0 atm. This specific pressure is recommended by Terumo Co. The length of the long axis is 2.0×10^{-2} m. The rated burst pressure (RBP) is 10.0 atm. The contrast media and physical saline solution were mixed in an equal ration and injected into the balloon using a syringe with a manometer.

2.2 Experimental Method

A stent was set up in the rotary table of the Micro-CT system using a syringe, and observations were made every 0.5 atm up to 8.0 atm over 5h. In this experimental system, the stent is not subject to external pressure. To examine the changes limited to the stent, the influence of external pressure was excluded. After reaching 8.0 atm, the balloon was deflated immediately and images were taken to evaluate ERS. 3D reconstruction and conversion to the STL format were performed using the software package VG Studio MAX 1.2.1 (NVS) and Magics 9.5.4 (Materialize, Japan).

ERS and eccentricity were calculated for quantitative reconstruction of stent expansion behavior. ERS was calculated using equation (1), where LD indicates the luminal diameter, subscript i indicate the proximal and distal positions and $LD_{i\_deflation}$ and $LD_{i\_8.0atm}$ represents LD_i at deflation and that at 8.0 atm pressure, respectively. Moreover, to determine the direction of ERS, equation (2) was introduced, where 2.5×10^{-3} m is the maximum diameter after expansion. Eccentricity (E) was evaluated according to equation (3) using d1 and d2. E is in the range of $0.0 \leq E \leq 1.0$, where the values close to 0.0, indicate a circle, and those close to 1.0, indicate a flat ellipse.

Elastic Recoil of Stent (ERS) equation

$$\mathrm{ER} = \frac{LD_{i\_deflation}}{LD_{i\_8.0\ atm}} \times 100 \quad \cdots (1)$$

where LD indicates the luminal diameter and i indicates the proximal and distal positions of each structural component.

Direction of ERS equation

$$\mathrm{ERS}_{direction} = \left(\frac{LD_{i\_8.0\ atm} - LD_{i\_deflation}}{2.5}\right) \times 100 \quad \cdots (2)$$

where LD indicates the luminal diameter and i indicates the proximal and distal positions of each structural component.

Eccentricity equation

$$\mathrm{E} = \frac{\sqrt{d_2^2 - d_1^2}}{d_2} \times 100 \quad \cdots (3)$$

where d1 is the diameter in the coronal view and d2 is the diameter in the sagittal view.

3. Results

3.1 Stent expansion behavior

The stent expansion behavior was observed using a reconstructed shape obtained from the Micro-CT images. Figure 4 shows the time-series expansion behavior of the stent

from 0.0 to 8.0 atm. At 0.0 atm, the diameter from the proximal point of structural component 1 to the distal point of structural component 6 was larger than that between the other structural components. No expansion was observed from 0.0 to 2.5 atm, but expansion from both ends began at 3.0 atm. Expansion clearly visible at 4.0 to 5.0 atm. From 5.0 to 8.0 atm, the stent expanded slowly. Figure5 shows the diameter increment curve of the stent from 0.0 to 8.0 atm and the diameter of the stent after deflation of the balloon. Several researches presented the behavior of stent expansion in the structure analysis using finite element method (FEM) and in-vitro. The behaviors of stent expansion in our results agree with these results [19-22]. The diameter of the stent at 8.0 atm was reduced compared with that after deflation of the balloon, called the elastic recoil of stent (ERS).

3.2 ERS

Figure 6 shows that ERS at 8.0 atm and that after deflation of the balloon overlapped, gray indicates the shape of stent at 8.0 atm and blue indicates the shape of the stent after deflation of the balloon. The stent size decreased in the directions shown by the red arrows.

ERS of each structural component was evaluated using equation (1). Figure 7 shows

the ERS ratio of d1 and d2 for each structural component. In d1, the smallest ERS ratio was 2.4 % at the distal point of the 2nd structural component, and the largest ERS ratio was 7.0 % at the distal point of the 6th structural component. On the other hand, in d2, the ERS ratio ranged from 3.8% in the proximal position of the 1st structural component to 9.2 % in the proximal position of the 4th structural component.

To determine the direction of ERS from the proximal and distal positions, equation (2) was introduced. The ERS ratio in the d1 direction was larger than that in the d2 direction from the proximal position of the 1st structural component and from the distal position of the 6th structural component. The maximum difference in ERS ratio between positions was 5.7% in the d2 direction from the distal position of the 2nd structural component. The minimum difference in ERS ratio was 0.8% in the d1 direction from the distal position of the 6th structural component.

3.3 Luminal eccentricity

Figure 8 indicates luminal eccentricity evaluated using equation (3). Various eccentricity values were observed for each structural component between 5.0 and 8.0 atm. The minimum eccentricity was 0.07 in the distal position of the 2nd structural component at 7.0 atm, and the maximum eccentricity was 0.59 in the proximal position

of the 5th structural component at 6.0 atm. Luminal eccentricity was not constant and was not close to a circular shape, even when the pressure was 8.0 atm (the specific pressure). Figure 9 shows a comparison of luminal eccentricity of the stent at 8.0 atm, that after deflation of the balloon, and that reported by Kawamori et al [23]. Kawamori et al. measured the maximum and minmum diameter of coronary stenosis by IVUS. They found that on cross-section, the eccentricity values could be represented by an ellipse before and after treatment and that the value did not represent a circle after stent implantation. Kawamori et al. reported luminal eccentricity of 0.44 both before and after treatment. On excluding the value from the proximal position of the 2nd structural component after deflation of the balloon, the luminal area of the stent at 8.0 atm was closer to the circular shape than that after deflation of the balloon. Moreover, the luminal eccentricity for the 3rd distal, 4th distal, 5th proximal, 5th distal and 6th proximal positions were larger than those measured by Kawamori et al. In these positions, the cross-section of the blood vessel may form more of an elliptical shape following stent placement and local stress.

3.4 Luminal Area

Figure 10 shows the luminal area of the stent at 8.0 atm and that after deflation of the

balloon. The luminal area ranged from 4.69×10^{-6} m^2 at the proximal position of the 1st structural component to 5.47×10^{-6} m^2 at the proximal position of the 3rd structural component at 8.0 atm. The luminal area of the stent after deflation of the balloon ranged from 4.29×10^{-6} m^2 at the distal position of the 1st structural component to 4.88×10^{-6} m^2 at the proximal position of the 3rd structural component. The greatest change of 13.5 % was observed from the 4 distal position of the 4th structural component. The smallest change of 7.6% was observed from the proximal position of the 1st structural component.

4. Discussion

DES is used for coronary stenosis. DES is embedded a drug in the strut and so the strut has complicated structures [24]. Then a local stress at stent expansion of this part can be estimated and the stress will lead asymmetric expansion.

We reconstructed STL files from images obtained using the Micro-CT system to observe the 3D expansion behavior of the test stent and to quantitatively evaluate its ERS. We found non-uniform stent expansion with different behaviors expressed by each of the structural components of the stent, indicating that 3D evaluation of ERS and expansion behavior are important.

Barragan et al. determined ERS using five points in the middle of a stent in 2D [11]. However, our results show that ERS ranged from 2.4 % to 9.2 % at the proximal and distal positions in 3D. When ERS was evaluated using the same method as Barragan et al., ERS was 4.0% in the coronal view and 6.7 % in sagittal view. The greatest difference in ERS between 2D and 3D values was 5.2 %, which would mean that half of the stent strut would have recoiled.

Yamamoto et al. evaluated the mean luminal area of an implanted stent by IVUS in 2D [5]. However, our results show that the luminal area in each structural component is not uniform during stent expansion and after ERS. After deflation of the balloon, the difference in the luminal area between the maximum and minimum values was 5.9×10^{-7} m^2 (ΔLD = 12 %), which would mean that moving 3 strut. This value differs from that obtained by measuring the cross-section. Luminal area after stent implantation is thought to be an important predictor of restenosis. The restenosis rate increase when the luminal area is small. If accurate information on stent behavior is not obtained, restenosis could occur. Therefore, it is important to determine the characteristic behavior of each type of stent, and these behaviors can be accurately measured in 3D not 2D.

In Otake H results[12], the higher average SEI decreased the frequency of uncovered

strut. Our results can show the minimum and maximum value of SEI from d1 and d2 were 0.82 at 5th proximal position and 0.99 at 3rd proximal position, respectively. Hence, it will be important to observe SEI in each part.

The stent used in the present study had a single–link structure. If the stent had a multi–link structure, the lumen cross-section might have approached a circular shape. Moreover, ERS of sing–link stents is greater than that of multi-link stents according to Barragan et al [11]. Thus ERS and eccentricity can also be classified on the basis of their link structure.

Barragan et al. also showed a lager ERS of coiled stents than of tubular stents [11]. However, only a tubular stent was assessed in the present study. Therefore, future studies should evaluate ERS and the structural characteristics of a coil stent in 3D. In addition, further research should focus on the effects of external pressure on stents because the values in this study represent minimum ERS value and eccentricity.

Conclusion

We reconstructed STL files from images obtained using a Micro-CT system to observed the 3D expansion behavior of a test stent and to quantitatively evaluate its ERS and eccentricity. Our results confirmed that 3D evaluation of expansion behavior and ERS

is necessary.

Acknowledgment

This study was supported by JSPS, Core-to-Core project, No.20001.

Reference

[1]Nobel A, Johnson R, Thomas A, Bass P, editors. The cardiovascular system: systems of the body. Elsevier Churchill Livingstone; 2005. p. 55-66.

[2]Serruys PW, de Jaeger P, Kiemeneij F, Macaya C, Rutsch W, Heyndrickx G, et al. A comparison of balloon-expandable-stent implantation with balloon angioplasty in patients with coronary artery disease. The New England Journal of Medicine. 1994; 331:489-495.

[3]Rensing BJ, Harmans WR, Strauss BH, et al. Regional differences in elastic recoil after percutaneous transluminal coronary angioplasty: A quantitative angiographic study. Journal of the American College of Cardiology. 1991; 17 (Suppl 6B):34B-38B.

[4]Rendoff A, Muma R. Evaluation of PTCA versus Stenting and Bare-Metal Stenting versus Drug-Eluting Stenting in the Treatment of Coronary Artery Disease. Proc. the 3rd Annual GRASP Symposium. 2007; 125-126.

[5]Yamamoto Y, Brown DL, Ischinger TA, Arbab-Zadeh A, Penny WF. Effect of Stent Design on Reduction of Elastic Recoil: A Comparison via Quantitative Intravascular Ultrasound. Catheterization and Cardiovascular Interventions. 1999; 47: 251-257.

[6] Tanimoto S, Serruys PW, Thuesen L, Dudek D, Bruyne B et al. Comparison of In Vivo Acute Stent Recoil Between the Bioabsorbable Everolimus-Eluting Coronary Stent and the Everolimus-Eluting Cobalt Chromium Coronary Stent: Insights From the ABSORB and SPIRIT Trials. Catheterization and Cardiovascular Interventions 2007; 70: 515-523.

[7] Serruys PW, Onumura Y, Omiston JA, de Bruyne B, Regar E et al. Evaluation of the Second Generation of a Bioresorbable Everolimus Drug-Eluting Vascular Scaffold for Treatment of De Novo Coronary Artery Stenosis : Six-Month Clinical and Imaging Outcomes. Circulation 2010; 122: 2301-2312.

[8]Kim BK, Ko YG, Oh S, Kim JS, Kang WC et al. Comparisons of the Effects of Stent Eccentricity on the Neointimal Hyperplasia between Sirolimus-Eluting Stent versus Paclitaxel-Eluting Stent. Yonsei Medical Journal 2010; 51: 823-831.

[9] Lemos P, Saia F, Ligthart J, Arampatzis C, Sianos G, Tanabe K et al. Coronary restenosis after sirolimus-eluting stent implantation: morphological description and mechanistic analysis from a consecutive series of cases. Circulation. 2003; 108:257–

260.

[10] Hwang CW, Wu D, Edelman ER et al. Physiological transport forces govern drug distribution for stent-based delivery. Circulation 2001; 104:600–605.

[11]Barragan P, Rieu R, Garitey V, Roquebert P, Sainsous J, Silvestri M, Bayet G. Elastic Recoil of Coronary Stents: A Comparative Analysis. Catheterization and Cardiovascular Interventions. 2000; 50:112-119.

[12] Otake H, Shite J, Ako J, Shinke T, Tanino Y et al. Local Determinants of Thrombus Formation Following Sirolimus-Eluting Stent Implantation Assessed by Optical Coherence Tomography. JACC Cardiovascular Interventions 2009; 2: 459-66.

[13] Sun Z, Allen YB, Mwipatayi BP, Hartley DE, Lawrence-Brown M. Multislice CT Angiography in the Follow-up of Fenestrated Endovascular Grafts: Effect of Slice Thickness on 2D and 3D Visualization of the Fenestration on Stents. Journal of endovascular therapy 2008; 15:417-426.

[14]Bouma BE, Tearney GJ, Yabushita H, Shishkov M, Kauffman CR et al. Evaluation of intracoronary stenting by intravascular optical coherence tomography. Heart 2003; 89: 317-320.

[15] Rieber J, Meissner O, Babaryka G, Reim S, Oswald M et al. Diagnostic accuracy of optical coherence tomography and intravascular ultrasound for the detection and

characterization of atherosclerotic plaque composition in ex-vivo coronary specimens: a comparison with histology. Coronary Artery Dis 2006; 17: 425-430

[16] Gurmeric S, Isguder GG, Carlier S, Unal G. A new 3-D automated computational method to evaluate in-stent neointimal hyperplasia in in-vivo intravascular optical coherence tomography pullbacks. Medical image computing and computer-assisted intervention 2009; 12:776-85.

[17]Ohta M, He C, Nakayama T, Takahashi A, Rüfenacht DA. Three-Dimensional Reconstruction of a Cerebral Stent using Micro-CT for Computational Simulation. Journal of Intelligent Material Systems and Structures. 2008; 19:313-318.

[18]Connolley T, Nash D, Buffière JY, Sharif F, McHugh PE. X-ray micro-tomography of a coronary stent deployed in a model artery. Medical Engineering & Physics. 2007; 29:1132-1141.

[19]Park WP, Cho SK, Ko JY, Kristensson A, Hassani STS et al. Evaluation of Stent Performances using FEA considering a Realistic Balloon Expansion. World Academy of Science, Engineering and Technology 2008; 37: 117-122.

[20]Wang WQ, Liang DK, Yang DZ, Qi YM. Analysis of the transientexpansionbehavior and design optimization of coronary stents by finite element method. Journal of Biomechanics 2006; 39: 21-32

[21]Wang YX, Yi H, Ni ZH. Experimental Research on Balloon-expandable Endovascular Stent Expansion. Proc. The 2005 IEEE Engineering in Medicine and Biology 27th Annual Conference 2005; 2272-2275.

[22]Kiousis DE, Wulff AR, Holzapfel GA. Experimental Studies and Numerical Analysis of the Inflation and Interaction of Vascular Balloon Catheter-Stent Systems. Annals of Biomedical Engineering 2009; 37: 315-330

[23]Kawamori H, Shite J, Shinke T, Otake H, Sawada T, Kato H, et al. The ability of optical coherence tomography to monitor percutaneous coronary intervention: detailed comparison with intravascular ultrasound. The Journal of Invasive Cardiology. 2010; 22:541-545.

[24]Abizaid A, Costa JR. New Drug-Eluting Stents An Overview on Biodegradable and Polymer-Free Next-Generation Stent Systems. Circulation Cardiovascular Interventions 2010; 3:384-393.

Tables

Table 1 Operating conditions of the Micro-CT system

Source of the focus X-ray parameter	50 [kv], 30[μA]
Field of view	$(2.5 \times 2.5 \times 2.2) \times 10^{-2}$ [m]
Raw data	512 × 512 [pixel]
Thickness	4.0×10^{-5} [m]

Figures

Fig.1 Schematic diagram of the Micro-CT system

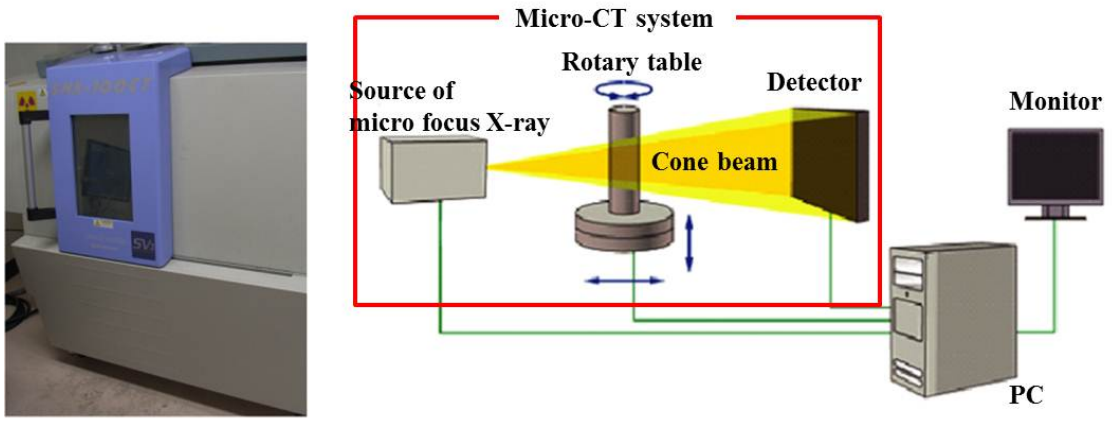

Fig.2 Terumo balloon-expanding coronary stent before expansion at 0.0 atm (upper panel), and after expansion at 8.0 atm (lower panel)

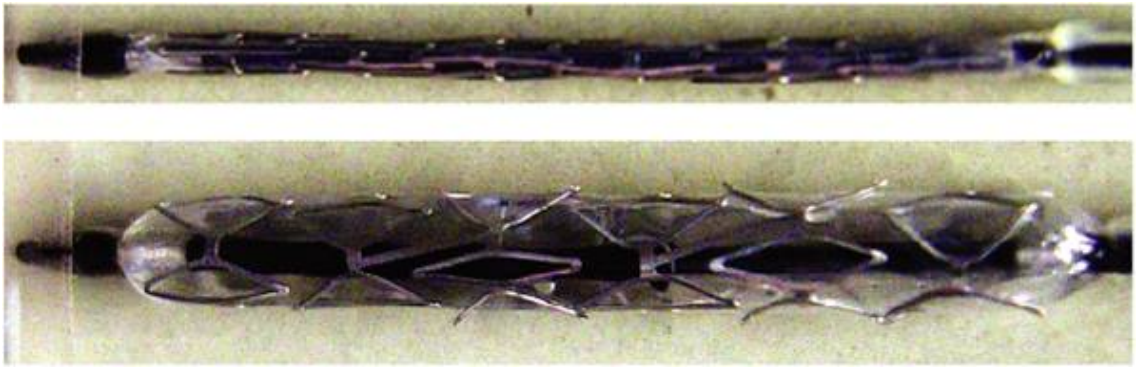

Fig.3 Structural components of the stent in a cross-section: This stent comprise 6 structural components, each of which is referred to by a number from 1 to 6. The

proximal and distal points at each ends of each structure are also shown. d1 in the coronal plane and d2 in the sagittal plane are connected to the opposite point in the cross-section of the stent shown here.

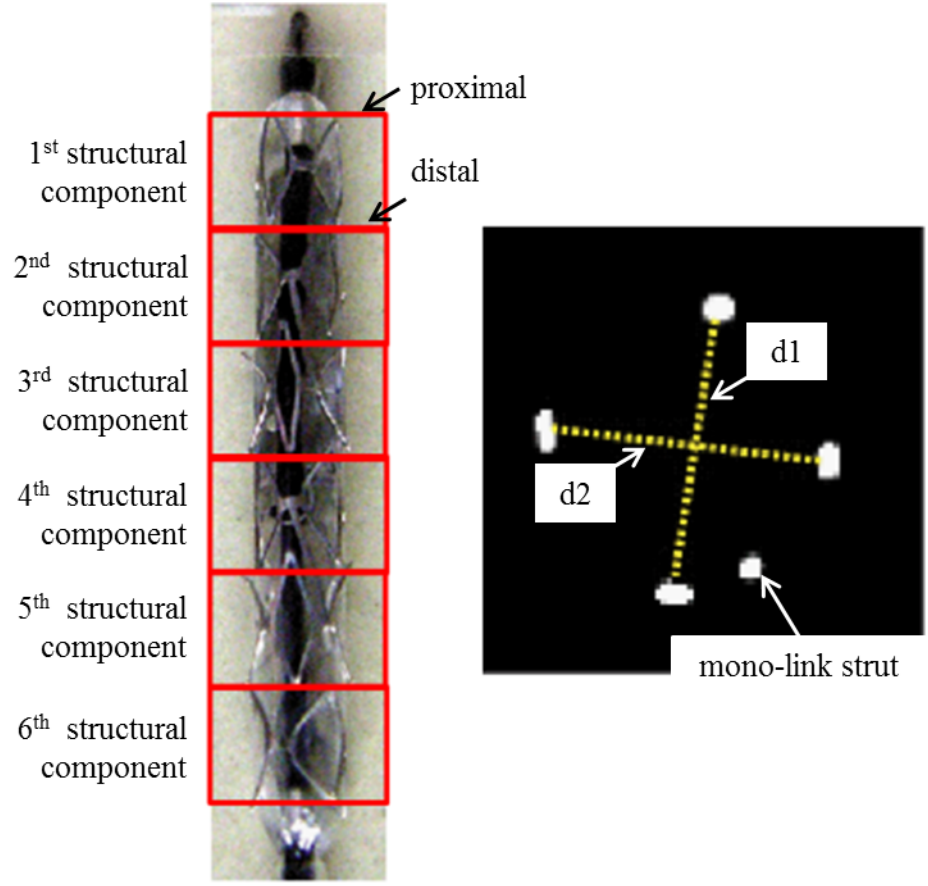

Fig.4 Stent expansion behavior at 0.0-8.0 atm (starting from the left: 0.0, 2.0, 4.0, 4.5, 5.0, 6.0, 8.0 atm)

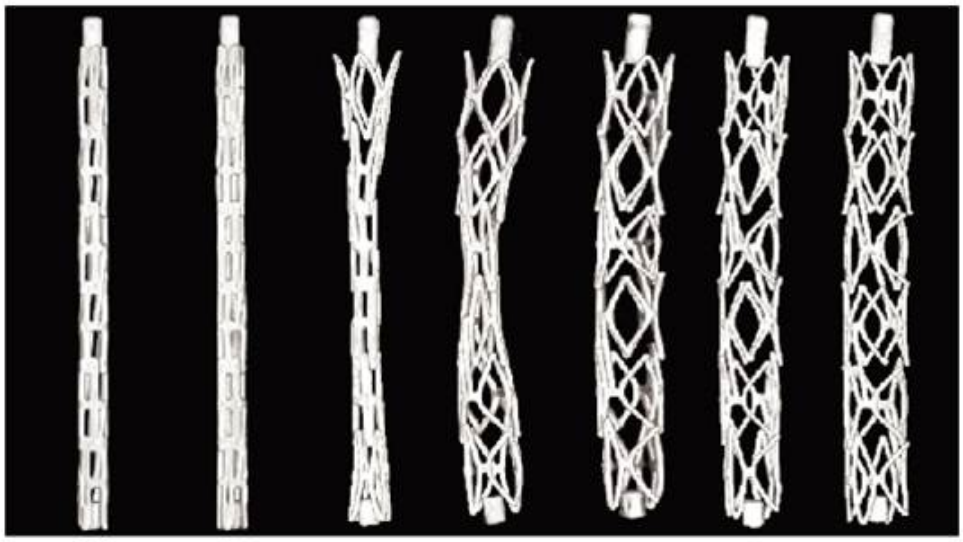

Fig.5 The diameter increment curve of the stent from 0.0 to 8.0 atm and that after deflation of the balloon at the proximal and distal positions of each structural component from 0.0 to 8.0atm: the X axis indicates pressure, and Y axis indicates the diameter.

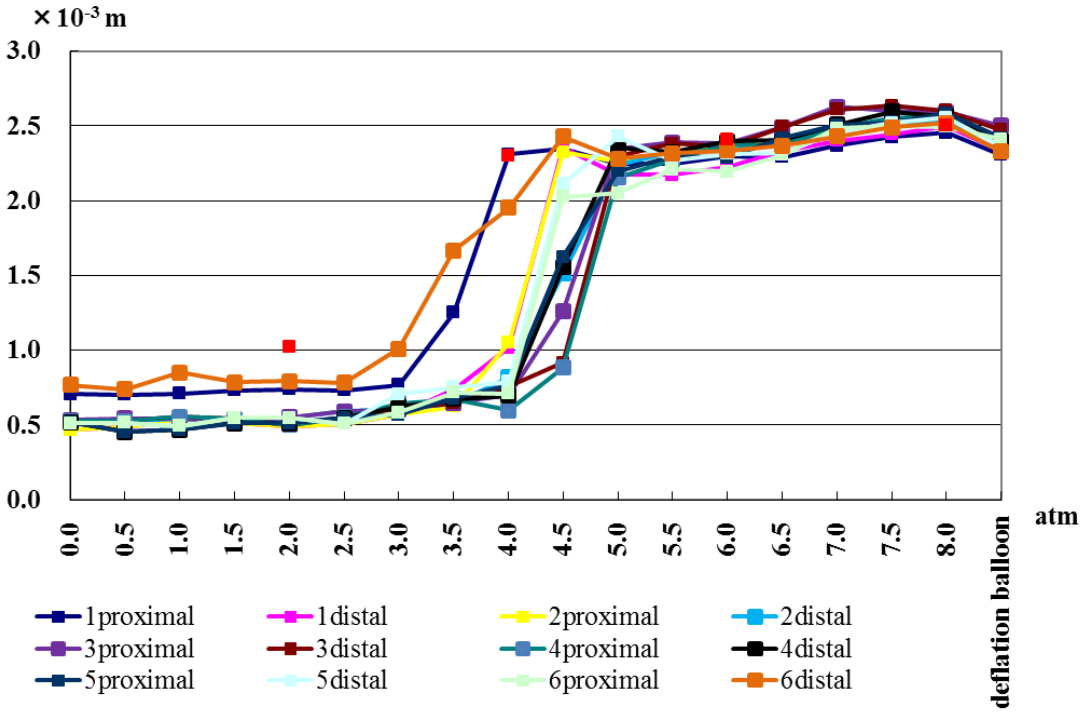

Fig.6 ERS at 8.0 atm overlapping with that after deflation of the balloon: The right image is a magnified view of the 3rd structural component. Gray indicates the position

at 8.0 atm, blue indicates deflation, and the red arrows indicates the direction of ERS

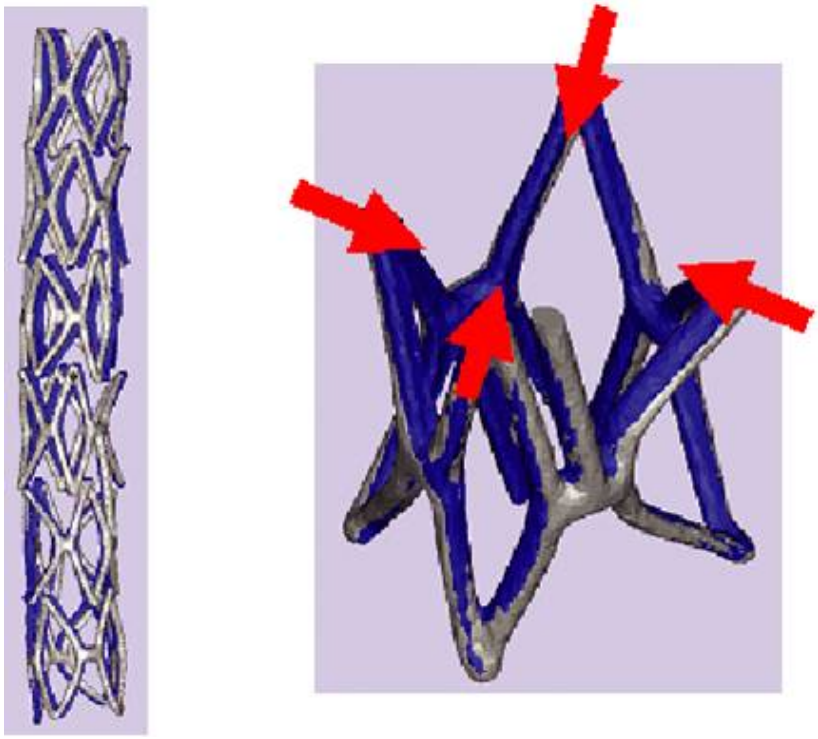

Fig.7 ERS ratio in d1 and d2 from the proximal and distal positions of each structural component: blue indicates d1 and red indicates d2. The X axis indicates each position, and Y axis indicates the ERS ratio.

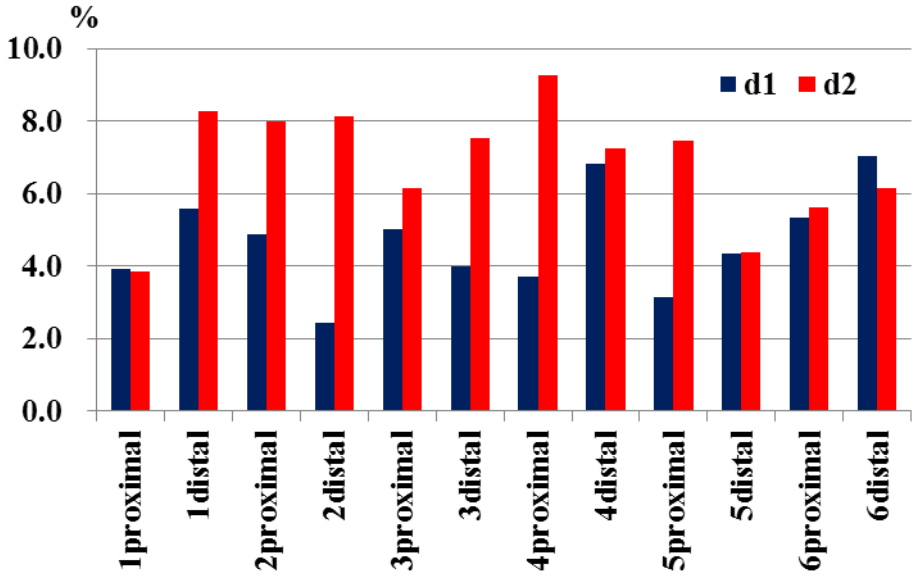

Fig.8 Luminal eccentricity at 5.0 to 8.0 atm: Blue 5.0 atm, Red 6.0 atm, Green 7.0 atm,

and Orange 8.0 amt. The X axis shows the position on each structural component, and the Y axis is the eccentricity (close to 0, a circle, and close to 1, a flat ellipse)

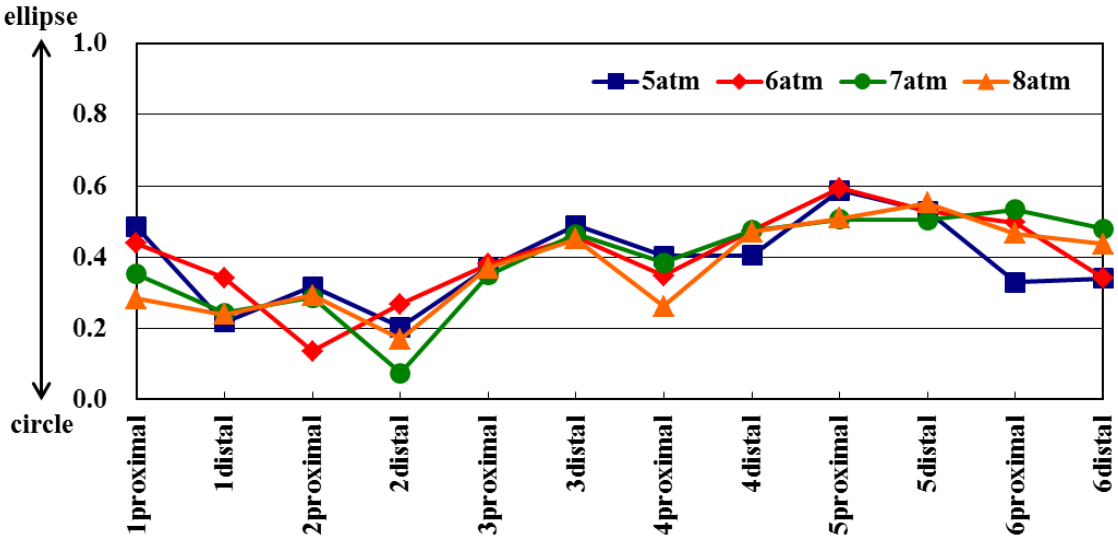

Fig.9 Comparison of luminal eccentricity of the stent at 8.0 atm, that after deflation of the balloon, and that reported by Kawamori et al. (blue, red, and green lines, respectively); The X axis indicates the position of each structural component, and the Y axis indicates the eccentricity (close to 0, a circle, and close to 1, a flat ellipse)

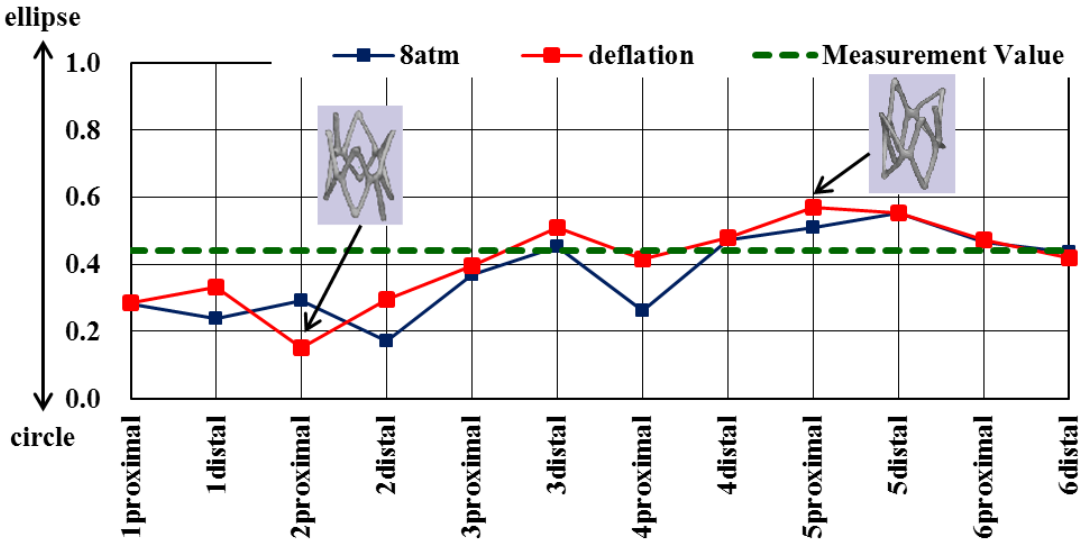

Fig.10 The luminal area of the stent at 8.0 atm and that after deflation of the balloon (blue and red, respectively). The X axis indicates the position of each structural component, the Y axis show the luminal area

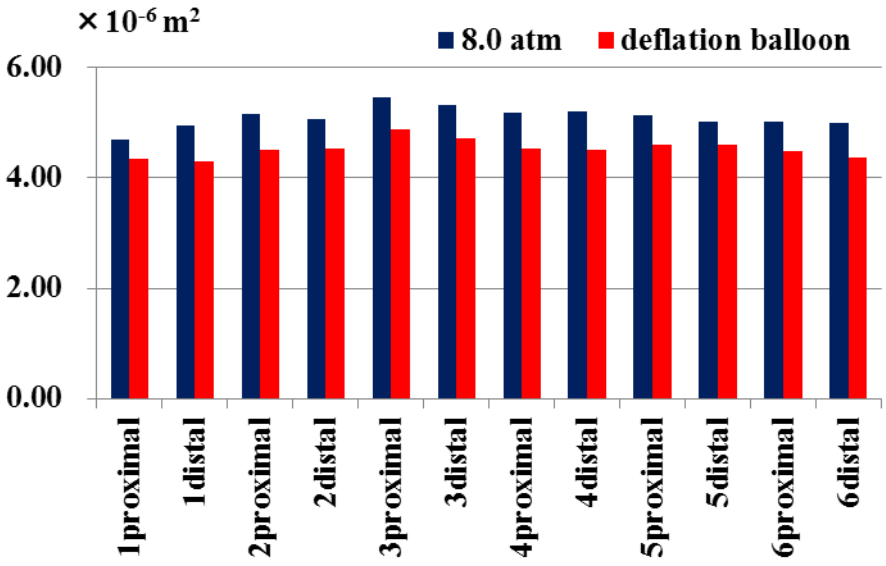
× 10-6 m2
8.0 atm
deflation balloon
6.00
4.00
2.00
0.00
1proximal
1distal
2proximal
2distal
3proximal
3distal
4proximal
4distal
5proximal
5distal
6proximal
6distal